2016 IEEE International Conference on Robotics and Automation (ICRA)
Stockholm, Sweden, May 16-21, 2016

Independent Control of Two Millimeter-Scale Soft-Bodied Magnetic Robotic Swimmers

Jiachen Zhang[1], Piyush Jain[2], and Eric Diller[1]

Abstract— **We present a method to independently control two millimeter-scale soft-bodied magnetic swimmers, with nominal dimensions of $1.5 \times 4.9 \times 0.06$ mm. A swimmer's speed depends on its relative angle with the actuation magnetic field. The two swimmers under control have different directions of net magnetic moments, and assume distinct orientations in one global magnetic field. With this fixed heading difference between two swimmers, the global actuation field forms different relative angles with the two swimmers. By manipulating these two relative angles, the two swimmers can exhibit different speeds. Theoretically, any speed ratios can be achieved between the two swimmers. In practice, a relatively accurate speed ratio can be obtained when both swimmers have nonzero speeds and one swimmer is no more than twice as fast as the other. Adding the control over the strength of actuation field, two swimmers can obtain independent speeds within a certain range. Two feedback controllers are proposed to control two such swimmers to arrive at independent global points (positioning) and move along paths (path following). Type I Sequential Controller manipulates two swimmers to move to their respective goals in sequence, while Type II Parallel Controller moves both swimmers simultaneously. Experiments are presented in which two swimmers are controlled to pass a series of points to form the letters "UT".**

I. INTRODUCTION

Tetherless mobile microrobots can perform tasks remotely in small and enclosed environments. Previous studies showed the wide range of potential applications of microrobots, including microobject manipulation and transportation [1], healthcare tasks [2], and scientific tools [3]. How to wirelessly control and actuate microrobots remains as an open-ended problem in the community of microrobotics. Many strategies have been proposed for this problem [4]–[6]. And using magnetic fields becomes a common choice. Magnetic fields can penetrate most materials, can exert both forces and torques on magnetic materials, and are easy and safe to generate and manipulate. Additionally, the setup to create magnetic fields using electric coils has a commonly followed standard, allowing different magnetic microrobots to be controlled by the same setup. Many microrobots have been proposed employing magnetic torques for actuation, some of which are soft-bodied microrobots [6]–[8]. Soft-bodied microrobots have distinct advantages over traditional rigid microrobots, including the ability of changing shape for propulsion, offering gentle interactions with their working environments, and being less prone to damages.

*This work is supported by the NSERC Discovery Grants Program.

[1]J. Zhang and E. Diller are with the department of Mechanical and Industrial Engineering, University of Toronto, 5 King's College Road, Toronto, M5S 3G8, Canada ediller@mie.utoronto.ca

[2]P. Jain is with the department of Mechanical Engineering, Indian Institute of Technology Kanpur, Kanpur, Uttar Pradesh 208016, India

The intrinsic small sizes of microrobots urge the research in controlling multiple microrobots to perform tasks in collaboration. An intuitive approach to control multiple microrobots is providing different localized signal to each individual. For example, up to ten opto-thermocapillary flow-addressed bubble (OFB) microrobots were manipulated by focusing laser beams into different patterns on a horizontal two-dimensional (2D) plane [9]. And two screw-type devices were propelled in their independent local magnetic fields created by a single magnetic dipole [10]. However, this method is difficult to be further scaled down because localized signals are more challenging to generate at a smaller resolution. Another option to control multiple microrobots for diverse behaviors, which doesn't have difficulties in being scaled down, is inducing a different response from each agent using the same global control signal. Differences in the magnetization strengths and geometric dimensions were utilized to configure three magnetic microrobots into independent global positions [11]. Other physical properties of microrobots, such as resonance frequencies, step-out frequencies, and turning-rates, have also been tested to differentiate an individual agent from a group [12]–[14].

This paper presents a new method to independently control two millimeter-scale soft-bodied magnetic swimmers. The concept of this swimmer was first reported in [6] and further characterized in [15] with preliminary results of controlling two swimmers. This swimmer can swim both at the air-water interface and in water [15]. This paper focuses on independently controlling the positions and the speed ratio of two swimmers. The two swimmers move at the air-water interface, and their speed ratio is defined as $\zeta = v_1/v_2$, where v_1 and v_2 are the speeds of the two swimmers, respectively. The proposed control strategy requires the net magnetic moments of the two swimmers to be neither parallel nor antiparallel. This method is able to manipulate two swimmers to achieve different speed values and move them to independent positions on a 2D horizontal plane, with the limitation that the relative angle between two swimmers' headings cannot be altered after fabrication. Two feedback controllers are proposed: Type I Sequential Controller and Type II Parallel Controller, which control two swimmers to move toward their respective goals in sequence or simultaneously. The theoretical problem of controlling multiple robots that moves in the same direction has been discussed in [16]. The work in this paper contributes to this problem as a specific implementation of controlling two robots moving at a fixed heading difference, with the study of methods to achieve different speeds.

978-1-4673-8026-3/16/$31.00 ©2016 IEEE

II. Concepts and Definitions

The swimmer in this work is composed of elastic polymer with magnetic particles. The magnetic particles are magnetized into a sinusoidal magnetization profile along the swimmer's body. When placed at the air-water interface inside uniform magnetic fields, the swimmer experiences magnetic torques, surface tension forces, and buoyancy, among which the magnetic torques play the dominating role in deforming the swimmer. The strength of actuation magnetic field is weaker than the coercivity of the magnetic particles, so the swimmers' magnetization will not be altered by the applied magnetic field. This section reviews the working principle of a single swimmer, which has been introduced in detail in [15], and lays the foundation for controlling two swimmers.

A. Principles of A Single Swimmer

The concept of the swimmer is depicted in Fig. 1. The two frames xyz and $x'y'z'$ are the global frame of the workspace and the local frame of the swimmer, respectively. As shown in Fig. 1(a), the swimmer has a sinusoidal magnetization profile $\mathbf{M}$ along its body with a constant magnitude and a rotating direction, which can be described by

$$\mathbf{M}(x') = M\cos\left(\frac{2\pi x'}{\lambda}\right)\hat{\mathbf{i}}' + M\sin\left(\frac{2\pi x'}{\lambda}\right)\hat{\mathbf{k}}', \qquad (1)$$

where M is the constant magnitude of magnetization, and λ is the wavelength of the sinusoidal magnetization profile. Vectors $\hat{\mathbf{i}}'$ and $\hat{\mathbf{k}}'$ are unit vectors of the local axes x' and z'. When placed in uniform magnetic fields, the swimmer's local magnetization forms a sinusoidally changing angle with the field, leading to magnetic torques with corresponding magnitudes. Together with the surface tension forces and buoyancy, the magnetic torques deform the swimmer's body into an approximate sinusoidal wave (Fig 1(b)). When the applied uniform magnetic field rotates in a vertical plane, the angles between the field and the swimmer's local magnetization change continuously, causing the swimmer's body to mimic a traveling wave and generate propulsive forces to make the swimmer swim (Fig 1(c)).

The wavelength λ is equal to the swimmer's length L, i.e., the swimmer has a full period of sinusoidal magnetization. Thus, the swimmer should have a zero net magnetic moment, i.e., $\int_0^L \mathbf{M}\mathrm{d}x' = \mathbf{0}$. However, a swimmer rarely has exactly zero net magnetic moment, due to inaccuracies in its fabrication process. The angle from a swimmer's positive x'-axis to the projection of its net magnetic moment on the x'-y' plane is defined as angle ϕ. Angle ϕ is either randomly determined or intentionally controlled by adding an extra magnetized portion to the swimmer's body (see [15]). Note that all angles and angle differences defined hereafter are automatically wrapped into the range of $(-\pi, \pi]$ for clarity. Utilizing the existence of this nonzero net magnetic moment, the swimmer's heading can be steered by a small constant magnetic field $\mathbf{B}_\mathrm{s}$ in the x-y plane. Hence, the magnetic field applied in the workspace is a superposition of a rotating field $\mathbf{B}_\mathrm{a}$ for actuation and a constant field $\mathbf{B}_\mathrm{s}$ for steering. As shown in Fig. 1(d), the direction of $\mathbf{B}_\mathrm{s}$ in the x-y plane is given by β_s, with respect to the positive x-axis. The direction of the rotating plane of $\mathbf{B}_\mathrm{a}$ is defined by a direction vector $\mathbf{e}_\mathrm{a}$ according to the right-hand-rule, whose direction in the x-y plane is given by angle β_a.

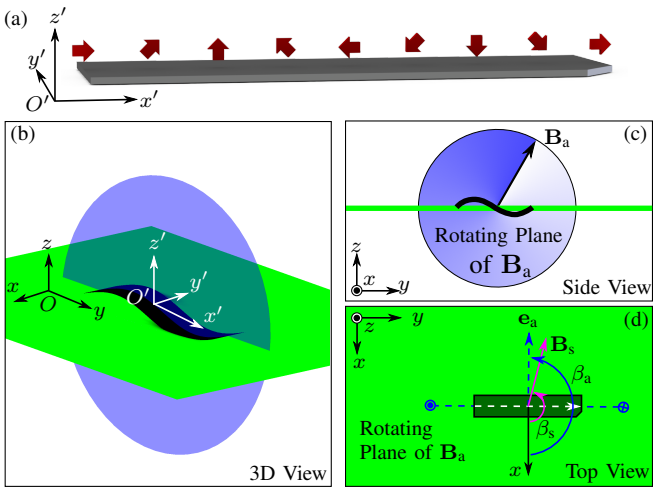

Fig. 1. Conceptual view of the swimmer with a sinusoidal magnetization profile, actuated by a rotating field $\mathbf{B}_\mathrm{a}$ and steered by a constant field $\mathbf{B}_\mathrm{s}$. A swimmer's model is shown in (a) together with arrows representing the magnetization direction along the swimmer's body. Views of a swimmer moving under the control of $\mathbf{B}_\mathrm{a}$ and $\mathbf{B}_\mathrm{s}$ are shown in (b), (c), and (d) from three different viewpoints. The actuation field $\mathbf{B}_\mathrm{a}$ rotates in a vertical plane that is denoted in blue. Whereas the steering field $\mathbf{B}_\mathrm{s}$ is applied in the horizontal plane that is colored in green.

B. Foundation for Controlling Two Swimmers

The proposed swimmers move in a non-holonomic fashion, i.e., they only move forward and backward along their x'-axes. A swimmer's speed is affected by its orientation relative to the vertical plane of the actuation field $\mathbf{B}_\mathrm{a}$. This orientation is described by an angle γ from the swimmer's local x' axis to the direction vector $\mathbf{e}_\mathrm{a}$ of field $\mathbf{B}_\mathrm{a}$, which is named the relative actuation angle, and calculated by

$$\gamma = \beta_\mathrm{a} - \beta_\mathrm{s} + \phi. \qquad (2)$$

A swimmer achieves its maximum positive and negative speeds when $\gamma = \pi/2$ and $-\pi/2$, respectively. In these cases, the plane of actuation field $\mathbf{B}_\mathrm{a}$ aligns with the swimmer and $\mathbf{B}_\mathrm{a}$ actually rotates in the swimmer's local x'-z' plane. As the plane of $\mathbf{B}_\mathrm{a}$ deviates from the swimmer's x'-z' plane, the magnitude of the swimmer's speed decreases. Fig. 2(a) shows the experimental data of three swimmers' speeds against their relative actuation angle γ, suggesting an approximate sinusoidal relationship between a swimmer's speed and γ, which can be expressed as

$$v(\gamma) = v_0\sin(\gamma), \qquad (3)$$

where v_0 is a nonzero scaling factor calculated by fitting the speed data to a sinusoidal curve. Thus, we can consider the swimmer's speed to be proportional to the maximum value of the projected magnitude of $\mathbf{B}_\mathrm{a}$ on the swimmer's x' axis.

For the case of two swimmers, the difference between the

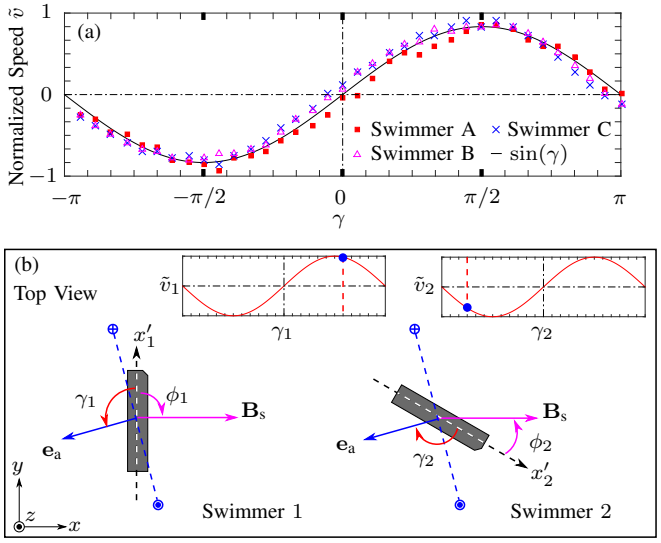

Fig. 2. Illustration of the foundation for controlling two swimmers. (a) The normalized speed $\tilde{v}$ of a swimmer varies with γ. The experimental data, which are average values of three trials, are shown together with a sinusoidal curve. The speed data of each trial is fitted with $v(\gamma) = v_0 \sin(\gamma)$ to determine v_0. The normalized speed is calculated as $\tilde{v} = v/v_0$. (b) Two swimmers with different directions of net magnetic moments ($\phi_1 \neq \phi_2$) assume different headings under the same steering field $\mathbf{B}_s$ and thus form different angles ($\gamma_1 \neq \gamma_2$) with the same global actuation field $\mathbf{B}_a$. The insets show the working points of each swimmer on its $\tilde{v}$ vs. γ graph.

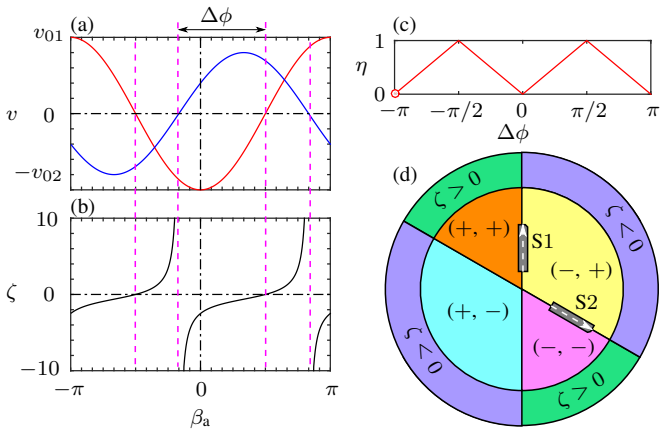

Fig. 3. Illustration of the speed ratio ζ of two swimmers and the controllability η. The speeds of swimmers S1 and S2, i.e., v_1 and v_2, are plotted against β_a in (a) as red and blue, respectively. The two swimmers' speed ratio $\zeta = v_1/v_2$ is shown in (b). (c) The value of controllability η is plotted against the heading difference between two swimmers $\Delta\phi$. (d) A circular plane is divided into four "quadrants" to illustrate the meaning of controllability η. The signs in parentheses mark the movement directions of two swimmers when direction vector $\mathbf{e}_a$ of $\mathbf{B}_a$ is within each quadrant: "+" means moving forward while "−" denotes swimming backward. The range of speed ratio ζ is labeled in the outer circle of each quadrant.

directions of their net magnetic moments is defined as the heading difference $\Delta\phi = \phi_2 - \phi_1$. When $\Delta\phi \neq 0$, the two swimmers assume different headings with an angle difference of $\Delta\phi$ in the same $\mathbf{B}_s$ field. Since the applied magnetic field is not strong enough to alter the swimmers' magnetization profiles, the orientation difference $\Delta\phi$ between two swimmers is a constant. Therefore, the same global actuation field $\mathbf{B}_a$ forms different relative actuation angles with the two swimmers, i.e., $\gamma_1 \neq \gamma_2$, resulting in different speeds from the two swimmers, as illustrated in Fig. 2(b). By controlling the directions and amplitudes of $\mathbf{B}_s$ and $\mathbf{B}_a$, different values of the speed ratio ζ between the two swimmers can be obtained.

This section reviews the basic working principles of swimmers and introduces the foundation for controlling two swimmers independently. For a more detailed characterization of a single swimmer's behavior, readers can refer to our previous work [6], [15]. In the next section, the capabilities and difficulties of this control method are characterized.

III. Characterization

This section characterizes the problem of controlling two swimmers. It is shown here that the two swimmers can theoretically achieve an arbitrary speed ratio ζ. Additionally, a variable η is defined to quantitatively measure the easiness of independently controlling two swimmers.

A. Speed Ratio and Values of Two Swimmers

As indicated in Fig. 2(a), a swimmer's speed v is sinusoidally dependent on its relative actuation angle γ. When two swimmers are in the same $\mathbf{B}_s$, the angle difference between their headings is $\Delta\phi$. If the two swimmers' speeds are plotted against β_a, the phase difference between the two curves is also $\Delta\phi$. To illustrate the relationship between the speeds of two swimmers, a swimmer S1 with $\phi_1 = -\pi/2$ and a swimmer S2 with $\phi_2 = \pi/6$ are taken as an example. It is also known that the speeds of S1 and S2 can be expressed by $v_1 = v_{01}\sin(\gamma_1)$ and $v_2 = v_{02}\sin(\gamma_2)$, respectively. When $\mathbf{B}_s$ is applied along the $+x$ direction, i.e., $\beta_s = 0$, the two swimmers' speeds are shown in Fig. 3(a) with respect to β_a. Fig. 3(b) shows the speed ratio ζ of two swimmers.

As shown in Fig. 3(b), ζ ranges from $-\infty$ to ∞, except when $\Delta\phi = 0$ or π, in which cases ζ can only be $0/0$ or v_{01}/v_{02}. By controlling the values of β_a and β_s, an arbitrary speed ratio ζ can be achieved theoretically. Nevertheless, limited by the noises in physical systems, an accurate speed ratio can be achieved only when both swimmers have nonzero speeds and one swimmer is no more than twice as fast as the other. It is also observed in experiments that a swimmer's speed increases with the strength of the magnetic field within an range. Therefore, independent speeds of the two swimmers, which are within the achievable range, can be realized by first obtaining the desired speed ratio and then scaling to the desired speeds.

B. Controllability

The preceding part has shown that two swimmers can achieve different speeds by choosing the appropriate input field angles β_a and β_s, as long as the directions of their net magnetic moments are neither parallel nor antiparallel, i.e., $\Delta\phi \neq 0$ or π. However, the level of difficulty in obtaining a desired speed ratio ζ in the presence of noises and errors varies with the value of $\Delta\phi$. To quantitatively evaluate

this level of difficulty, a variable η named controllability is defined as

$$\eta = \frac{2 \times \min\left(|\Delta\phi|,\, \pi - |\Delta\phi|\right)}{\pi}, \tag{4}$$

where function min() returns the minimum value of its two inputs. The value of η is plotted against $\Delta\phi$ in Fig. 3(c), which suggests that a two-swimmer set with $\Delta\phi = \pm\pi/2$ has the highest controllability ($\eta = 1$, easiest to control independently) while a set with $\Delta\phi = 0$ or π has the lowest controllability ($\eta = 0$, impossible to control independently).

The meaning of η can be intuitively perceived from Fig. 3(d), in which a circular plane is divided into four parts by the local x'-axes of two swimmers, similar with the four quadrants of a coordinate frame. Diagonal quadrants correspond to the same range of speed ratio ζ. In the case of $\Delta\phi = \pm\pi/2$, the four quadrants have identical areas. Otherwise, two diagonal quadrants are compressed while the other two being expanded. When the areas of a pair of diagonal quadrants are compressed, ζ in the corresponding range becomes more sensitive to the change of the direction of $\mathbf{B}_\mathrm{a}$, resulting in a higher requirement on the input accuracy and a lower value of the controllability η. In the uncontrollable cases ($\Delta\phi = 0$ or π), this four-quadrant structure collapses into a two-quadrant one, and the two swimmers have two fixed ζ value, i.e., $0/0$ and v_{01}/v_{02}, whichever direction $\mathbf{B}_\mathrm{a}$ is applied, resulting in $\eta = 0$. Thus, the relative angle $\Delta\phi$ between the two swimmers' net magnetic moments affects the level of difficulty in controlling two swimmers independently, which is described by the value of η. The most desirable case is when two swimmers have perpendicular magnetic moments, i.e., $\Delta\phi = \pm\pi/2$, while the worst case happens when the net magnetic moments of two swimmers are parallel or antiparallel, i.e., $\Delta\phi = 0$ or π.

IV. Feedback Controllers

Based on the capability of inducing independent speeds from two swimmers, two controllers are designed to independently position two swimmers at a horizontal plane. Since the relative heading difference $\Delta\phi$ of two swimmers is a fixed value, the two swimmers cannot move directly toward their respective goals simultaneously in most cases. The two controllers proposed here solve this problem in two distinct ways: one controller moves one swimmer at a time, while the other controller actuates two swimmers to zigzag toward their respective goals simultaneously.

A. Navigation and Control Geometry

Two fictitious swimmers S1 and S2 with $\phi_1 = \pi/12$ and $\phi_2 = \pi/2$ are drawn in Fig. 4 to illustrate the related definitions. Points P and G stand for the present and goal positions of a swimmer, respectively. Goal vector $\mathbf{r}$ points from point P to G. Swimmer S1 (S2) can be brought into alignment with $\mathbf{r}_1$ ($\mathbf{r}_2$) by a steering field $\mathbf{B}_\mathrm{s}$ applied along the line l_1 (l_2). Since a swimmer can move both forward and backward, the field $\mathbf{B}_\mathrm{s}$ can be applied along either direction of line l_1 (l_2). If l_1 coincides with l_2, S1 and S2 will align with their respective goal vectors simultaneously when $\mathbf{B}_\mathrm{s}$ is along l_1 or l_2. In this case, the two controllers produce the same result: The two swimmers move directly toward their goals simultaneously in straight lines. By selecting the direction of $\mathbf{B}_\mathrm{a}$, the velocities of two swimmers are regulated so that both swimmers reach their goals at the same time. When l_1 does not coincide with l_2 (as is shown in Fig. 4), S1 and S2 are not able to align with $\mathbf{r}_1$ and $\mathbf{r}_2$ simultaneously, no matter which direction $\mathbf{B}_\mathrm{s}$ is applied. This is the case in which the two controllers perform differently.

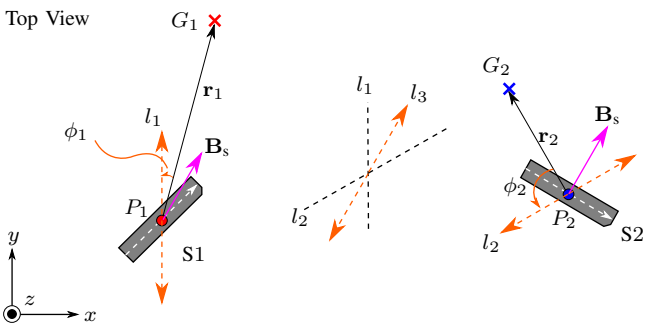

Fig. 4. Definitions of related variables for the proposed two controllers.

B. Type I Sequential Controller

When l_1 does not coincide with l_2, Type I Sequential Controller controls the two swimmers to reach their respective goals in sequence. This controller first compares the two swimmers's distances to their respective goal positions, i.e., $|\mathbf{r}_1|$ and $|\mathbf{r}_2|$. Then, $\mathbf{B}_\mathrm{s}$ is applied in a direction so that the swimmer with a longer distance (S1 in the example) aligns with its goal. And the direction vector $\mathbf{e}_\mathrm{a}$ of $\mathbf{B}_\mathrm{a}$ is aligned with the other swimmer S2 ($\gamma_2 = 0$), so that the actuation field rotates in a plane that is perpendicular to the local x' axis of S2. Consequently, $\mathbf{B}_\mathrm{a}$ only propels S1 to move toward its goal, while keeping S2 stationary. After S1 has reached its goal, $\mathbf{B}_\mathrm{s}$ and $\mathbf{B}_\mathrm{a}$ are changed to align S2 with its goal and make S2 move and S1 stop.

C. Type II Parallel Controller

When both swimmers need to move, i.e., $|\mathbf{r_1}| \cdot |\mathbf{r_2}| \neq 0$, Type II Parallel Controller manipulates two swimmers in parallel. This controller selects the directions of $\mathbf{B}_\mathrm{s}$ and $\mathbf{e}_\mathrm{a}$ so that $|\mathbf{r_1}|$ and $|\mathbf{r_2}|$ are reduced simultaneously and in a balanced manner. When l_1 and l_2 are not colinear, $\mathbf{B}_\mathrm{s}$ is selected to be along the angle bisector l_3 of the smaller angle formed by l_1 and l_2 (Fig. 4). This choice is a compromise that minimizes the sum of the deviation angles of S1 and S2 from $\mathbf{r}_1$ and $\mathbf{r}_2$, and makes the two deviation angles equal to each other. The decision of which side of l_3 to use as the new $\mathbf{B}_\mathrm{s}$ is based on the criterion that the change between the new and the previous directions of $\mathbf{B}_\mathrm{s}$ should be minimized.

After the direction of $\mathbf{B}_\mathrm{s}$ is selected, the controller selects the direction vector $\mathbf{e}_\mathrm{a}$ of $\mathbf{B}_\mathrm{a}$ such that the speed ratio of two swimmers is equal to their distance ratio, i.e.,

$$\zeta = \frac{|\mathbf{r}_1|}{|\mathbf{r}_2|} = \frac{|v_{01}\sin(\gamma_1)|}{|v_{02}\sin(\gamma_2)|} = \frac{v_{01}|\sin(\gamma_1)|}{v_{02}|\sin(\Delta\phi + \gamma_1)|}. \tag{5}$$

For two controllable swimmers, $\sin(\Delta\phi) \neq 0$, and it is also known that $|\mathbf{r_1}| \cdot |\mathbf{r_2}| \neq 0$, we can get

$$\gamma_1 = \cot^{-1}\left(\frac{\pm\frac{|\mathbf{r}_2|v_{01}}{|\mathbf{r}_1|v_{02}} - \cos(\Delta\phi)}{\sin(\Delta\phi)}\right). \tag{6}$$

The variable γ_1 has four values from (6), corresponding to the four possible combinations of the two swimmers' moving directions. Only one of the four γ_1 values corresponds to the movement that reduces both swimmers' distances to their goals, and this γ_1 value is used to determine the rotation direction of $\mathbf{B}_\mathrm{a}$ as $\beta_a = \beta_\mathrm{s} - \phi_1 + \gamma_1$.

D. Compatibility with Path Following Tasks

Although both controllers are designed for the independent positioning of two swimmers and only consider the swimmers' final positions, these two controllers are compatible with path following tasks, with the desired path being approximated by line segments. For Type I Sequential Controller, the swimmers move in straight lines and their deviations from desired paths is negligible. Under Type II Parallel Controller, swimmers zigzag toward their goals with relatively large and fluctuating deviations. Thus, a deviation limiter is imposed on Type II Parallel Controller for path following tasks.

V. Experimental Demonstrations

This section briefly introduces the fabrication procedures and experimental setups for swimmers (more details in [15]), and present the experimental results of the proposed two controllers and the deviation limiter.

A. Fabrication of Swimmers and Experimental Setup

Swimmers are composed of elastomer (Ecoflex 00-50, density 1.07 g/cm^3, Young's modulus 83 kPa) with unmagnetized magnetic powders (MQFP-15-7, NdPrFeB, Magnequench) mixed at a mass ratio of 1:1. A elastomer sheet cures in a gap of 0.06 mm between two acrylic plates. Swimmers are cut from the cured sheet by a laser cutter (Epilog Laser Mini 40 Watt) with nominal dimensions of 1.5×4.9 mm. Rolled into circles, swimmers are magnetized in a uniform magnetic field (1 T), which programs a sinusoidal magnetization profile into the swimmers' bodies. The experimental setup includes an electromagnetic coil system with three pairs of wire loops and three analog servo drives (30A8, Advanced Motion Controls), a multifunction analog/digital I/O board (Model 826, Sensoray), a 60 fps camera (FO134TC, FOculus) mounted atop the workspace, and a computer with custom programs. Each pair of wire loops is arranged in an approximate Helmholtz configuration, resulting in a uniform magnetic field up to 15 mT in the workspace located at the geometric center of the coil system.

B. Demonstrations of Two Controllers

Two swimmers, S1 with $\phi_1 = 127°$ and S2 with $\phi_2 = -164°$, are controlled to pass a series of goal points along letters "UT" to demonstrate the efficacies of the two controllers, whose results are shown in Fig. 5. With Type I Sequential Controller, only one swimmer moves at a time, swimming toward its goal in a straight line. Thus, the distance traveled by each swimmer is minimized. The moving swimmer does not necessarily swim at its maximum speed, because the rotation direction of actuation field is aligned with the other swimmer to keep it stationary. For Type II Parallel Controller, both swimmers zigzag simultaneously to their respective goals. Since this controller does not consider the swimmers' deviations, the two swimmers deviate obviously from the desired path, as shown in Fig. 5(b).

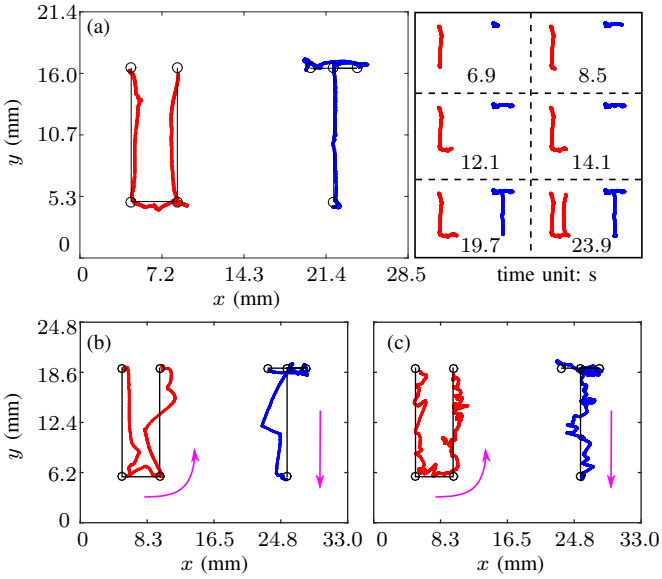

Fig. 5. Paths of two swimmers in "UT" following experiments. Goal points and desired paths are marked by black circles and lines, respectively. Center points of two swimmers are represented by red (S1) and blue (S2) dots. Results of Type I Sequential Controller are shown in (a) with small figures illustrating the moving order of swimmers. Results of Type II Parallel Controller without a deviation limiter are plotted in (b). Swimmers' paths under the control of Type II Parallel Controller and a deviation limiter with $\rho = 0.05$ bl. are shown in (c). Video is available in supplementary materials.

C. Type II Parallel Controller with Deviation Limiter

Adding a deviation limiter, Type II Parallel Controller can work for path following tasks, with the desired path being approximated by line segments. The goal points for swimmers are the connecting points of these line segments. Before the swimmers begin to move toward the next group of connecting points of line segments, the deviation limiter predicts the next turning points of the two swimmers. If at least one turning point is outside the allowable deviation range ρ, the limiter re-positions the turning points so that both of them are within ρ. Then, the deviation limiter passes the two turning points to Type II Parallel Controller as its next goal points. After both swimmers have arrived at the goal points specified by the deviation limiter, the limiter specifies next group of intermediate goal points, until two swimmers reach their "original" goal points, i.e., the connecting points of line segments. Thus, the actual deviations of two swimmers are limited within a range, as shown in Fig. 5(c).

The deviation limiter is characterized by studying the

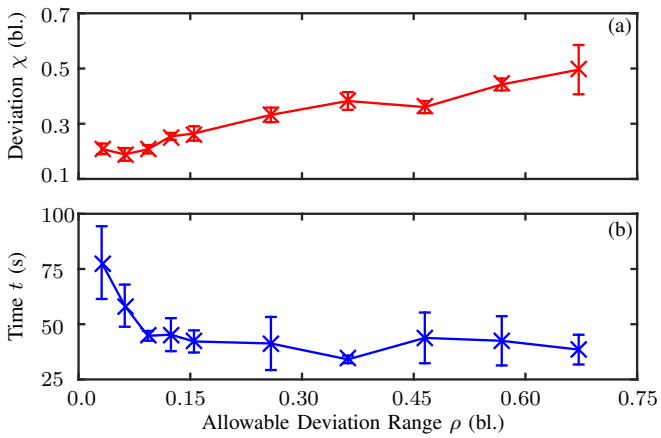

Fig. 6. Experimental data showing the effect of the allowed deviation range ρ on the total deviation χ (a) and the path completion time t (b). Five trials are performed for each data point using the two swimmers introduced in previous experiments.

effect of ρ on χ and t, where χ is the root-mean-square (rms) value of the sum of two swimmers' deviations from the desired paths and t is the path completion time taken by the two swimmers to both arrive at goals. As shown in Fig. 6(a), the total deviation χ increases with the allowable deviation range ρ, proving the efficacy of the limiter. However, χ does not go to zero with ρ because swimmers zigzag toward their goals and swimmers drift every time they turn. On the other end of the curve, χ does not increase infinitely with ρ, because the deviations of two swimmers are limited by the controller even without the deviation limiter. The effect of ρ on the time t is more complicated. In general, the swimmers need more time when the allowable deviation range ρ is smaller, as a result of more turns required. However, the time used by making turns is only one part of the total time consumed, and a large amount of time will be taken if a relatively large drifting happens. Therefore, t is less sensitive to ρ and has a relative large standard deviation than χ.

VI. Conclusions

This paper studies the problem of independently controlling two swimmers using a global magnetic field. Two swimmers with net magnetic moments that point in different directions can be controlled to achieve an arbitrary speed ratio. Based on this, independent positioning of two swimmers is achieved using two computer vision-based feedback controllers: Type I Sequential Controller and Type II Parallel Controller. Type I Sequential Controller manipulates swimmers to move toward their goals one after another, while Type II Parallel Controller moves both swimmers to zigzag toward their goals simultaneously. Two swimmers are controlled to pass a series of goal points defined along the letters "UT", which demonstrates the efficacies and characteristics of the two controllers. Swimmers under the control of Type I Sequential Controller do not deviate much from straight lines, while the deviations of swimmers with Type II Parallel Controller go up and down whilst swimmers move toward their goals. A deviation limiter to restrain the deviations of swimmers with Type II Parallel Controller is implemented for path following tasks, and is characterized with respect to total deviation and path completion time.

This paper only explores the problem of independently controlling two swimmers. For more swimmers, the proposed method does not apply directly, limited by the fact that the heading difference between swimmers' net magnetic moments is fixed. In our experiments, a large distance is kept between the two swimmers, such that the local interaction between swimmers is negligible. Some experimental results suggest that the behavior of swimmers with strong local interactions can still be modulated. Future research will investigate the problem of manipulating swimmers in close proximity with each other, and completing useful tasks using a team of swimmers.

References

[1] Z. Ye, E. Diller, and M. Sitti, "Micro-manipulation using rotational fluid flows induced by remote magnetic micro-manipulators," *J. Appl. Phys.*, vol. 112, no. 6, 2012.

[2] B. Nelson, I. Kaliakatsos, and J. Abbott, "Microrobots for minimally invasive medicine." *Annu. Rev. Biomed. Eng.*, vol. 12, pp. 55–85, 2010.

[3] M. Sakar, E. Steager, A. Cowley, V. Kumar, and G. Pappas, "Wireless manipulation of single cells using magnetic microtransporters," in *IEEE Int. Conf. on Robotics and Automation*, 2011, pp. 2668–2673.

[4] A. Solovev, W. Xi, D. Gracias, S. Harazim, C. Deneke, S. Sanchez, and O. Schmidt, "Self-propelled nanotools," *ACS Nano*, vol. 6, no. 2, pp. 1751–1756, 2012.

[5] B. Behkam and M. Sitti, "Effect of quantity and configuration of attached bacteria on bacterial propulsion of microbeads," *Appl. Phys. Lett.*, vol. 93, no. 22, 2008.

[6] E. Diller, J. Zhuang, G. Lum, M. Edwards, and M. Sitti, "Continuously distributed magnetization profile for millimeter-scale elastomeric undulatory swimming," *Appl. Phys. Lett.*, vol. 104, no. 17, 2014.

[7] I. Khalil, H. Dijkslag, L. Abelmann, and S. Misra, "MagnetoSperm: A microrobot that navigates using weak magnetic fields," *Appl. Phys. Lett.*, vol. 104, no. 22, 2014.

[8] R. Dreyfus, J. Baudry, M. Roper, M. Fermigier, H. Stone, and J. Bibette, "Microscopic artificial swimmers," *Nature*, vol. 437, pp. 862–865, 2005.

[9] W. Hu, Q. Fan, and A. Ohta, "Interactive actuation of multiple opto-thermocapillary flow-addressed bubble microrobots," *Robotics Biomim.*, vol. 1, no. 1, 2014.

[10] N. D. Nelson and J. J. Abbott, "Generating Two Independent Rotating Magnetic Fields with a Single Magnetic Dipole for the Propulsion of Untethered Magnetic Devices," in *IEEE Int. Conf. on Robotics and Automation*, 2015, pp. 4056–4061.

[11] S. Floyd, E. Diller, C. Pawashe, and M. Sitti, "Control methodologies for a heterogeneous group of untethered magnetic micro-robots," *Int. J. Robot. Res.*, vol. 30, no. 13, pp. 1553–1565, 2011.

[12] B. Kratochvil, D. Frutiger, K. Vollmers, and B. Nelson, "Visual servoing and characterization of resonant magnetic actuators for decoupled locomotion of multiple untethered mobile microrobots," in *IEEE Int. Conf. on Robotics and Automation*, 2009, pp. 1010–1015.

[13] A. Mahoney, N. Nelson, K. Peyer, B. Nelson, and J. Abbott, "Behavior of rotating magnetic microrobots above the step-out frequency with application to control of multi-microrobot systems," *Appl. Phys. Lett.*, vol. 104, 2014.

[14] I. Paprotny, C. Levey, P. Wright, and B. Donald, "Turning-rate Selective Control: A New Method for Independent Control of Stress-engineered MEMS Microrobots," in *Robotics: Science and Systems VIII*, 2013, pp. 321–328.

[15] J. Zhang and E. Diller, "Millimeter-Scale Magnetic Swimmers Using Elastomeric Undulations," in *IEEE/RSJ Int. Conf. on Intelligent Robots and Systems*, 2015.

[16] T. Bretl, "Minimum-time optimal control of many robots that move in the same direction at different speeds," *IEEE Trans. Robot.*, vol. 28, no. 2, pp. 351–363, 2012.